Stanford Exploration Project, Report 100, April 20, 1999, pages 135–141

Short Note

Comparing Kirchhoff with wave equation migration in a hydrate region

Mamta Sinha and Biondo Biondi[1]

keywords: *kirchhoff, wave-equation*

INTRODUCTION

Prestack migration is necessary before AVO analysis. Most of the present migration algorithms not only try to focus the reflections on the subsurface but also strive to preserve the amplitude for subsequent amplitude studies. A migration/inversion method developed by Lumley (1993) estimates the angle dependent reflectivity at each subsurface point by using least-squares Kirchhoff migration followed by a linearized Zoeppritz elastic parameter inversion for relative contrasts in compressional and shear wave impedance. Another migration algorithm is based on the wave-equation method which uses the Double Square Root equation (DSR) for downward continuation. Migration methods based on DSR operators have been applied to 2-D prestack migration for a long time (Claerbout, 1984) . Only recently computationally efficient methods to continue 3-D prestack data have been presented (Biondi and Palacharla, 1995). The objective of this paper is to compare the results of the above two algorithms.

The data are taken from the gas hydrate region in Blake Outer Ridge on offshore Florida In a previous study (Ecker, 1998), the prestack migration is performed with the Kirchhoff migration/inversion. In this paper the same prestack data is migrated by the DSR wave-equation migration as explained in Prucha et al(1999).

COMPARISON

Although the goal of both Kirchhoff and wave-equation migration is to properly image the subsurface, they differ in many ways. The first difference is that the two migrations are in separate domains. The Kirchhoff migration is in the offset domain and the wave-equation migration is in the angle domain (Prucha et al., 1999). The stacked section obtained by Kirchhoff migration is shown in Figure 3. It shows the BSR quite clearly and also images

[1]**email:** mamta@sep.stanford.edu, biondo@sep.stanford.edu

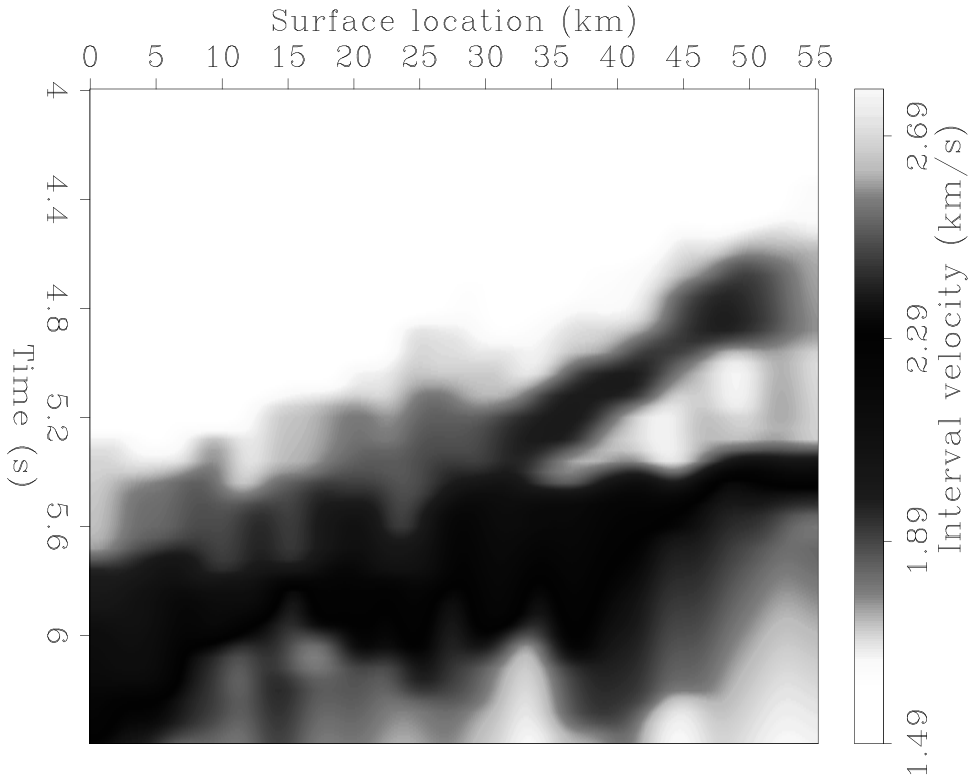

Figure 1: The velocity model used for the two migration methods. mamta2-Vel-hydrate-paper [CR]

a relatively flat reflector beneath the BSR which seems to fade as it approaches the BSR and completely vanishes near the BSR. The same section after wave-equation migration (Figure 4) also images the BSR equally well but better resolves the reflector below the BSR. It is continuous and cuts across the BSR. Though the energy of the reflection still decreases towards the BSR it does not vanish. The latter image has a higher frequency content which shows up as the sharpness of the reflectors.

Constant image gathers are then compared to observe the accuracy of the two methods in resolving the BSR from the layer below. Figure 2 shows the two image gathers at a large distance from the crossing of the BSR with the flat layer. The results are qualitatively similar including the discontinuity in the reflectors. This discontinuity results because of the acquisition geometry, the near offset being double the far offset. It has spread out on the reflection angle gather so is faintly visible there. Figures 5 and 6 are at CMPs 37.5 km and 33.5 km respectively, where the lateral velocity variation is stronger, the wave-equation migration clearly resolves the two reflectors whereas the lower layer vanishes for the Kirchhoff migration.

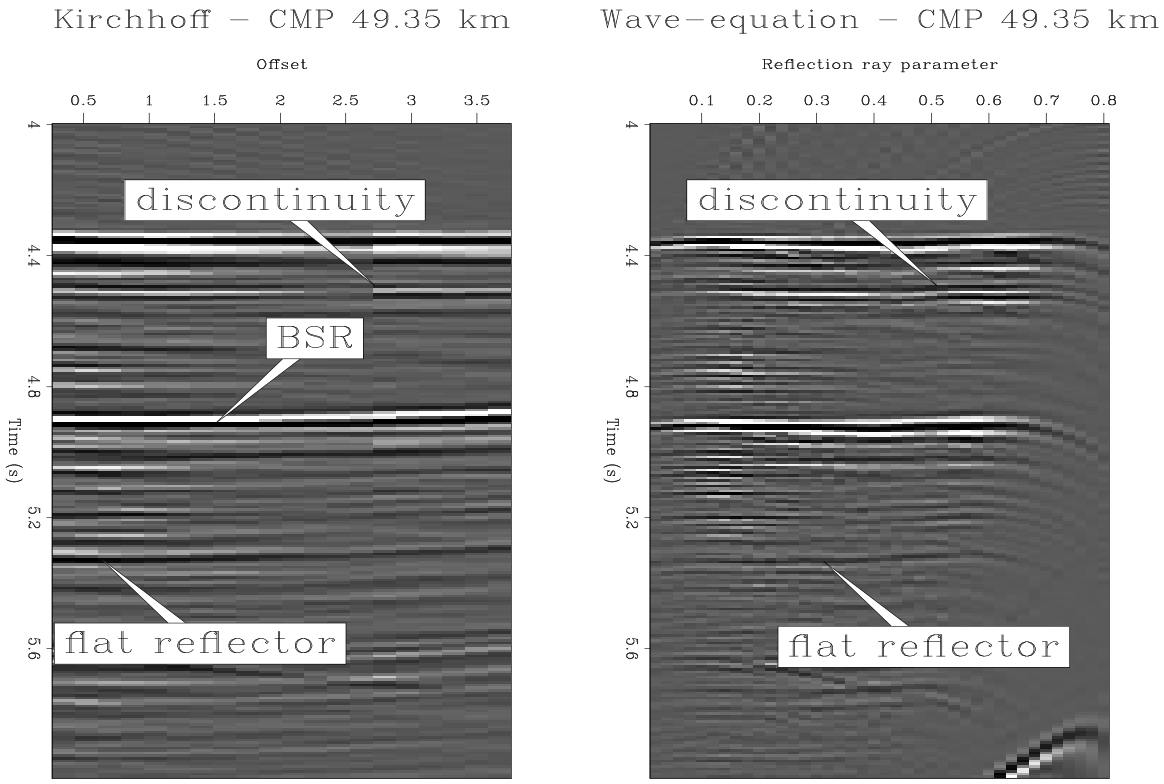

Figure 2: Common midpoint gather at 49.35 km. mamta2-AVO-49.35-ann [CR]

DISCUSSION AND FUTURE WORK

The above comparisons lead us to hypothesize that wave-equation migration can yield more accurate estimates of reflectors' amplitudes in places of lateral velocity variation. Since it

now images the lower layer below the BSR, it encourages us to study it in detail. The fact that it fades away as it approaches the BSR could lead to some interesting results. It would enable us to do an amplitude analysis of this particular layer.

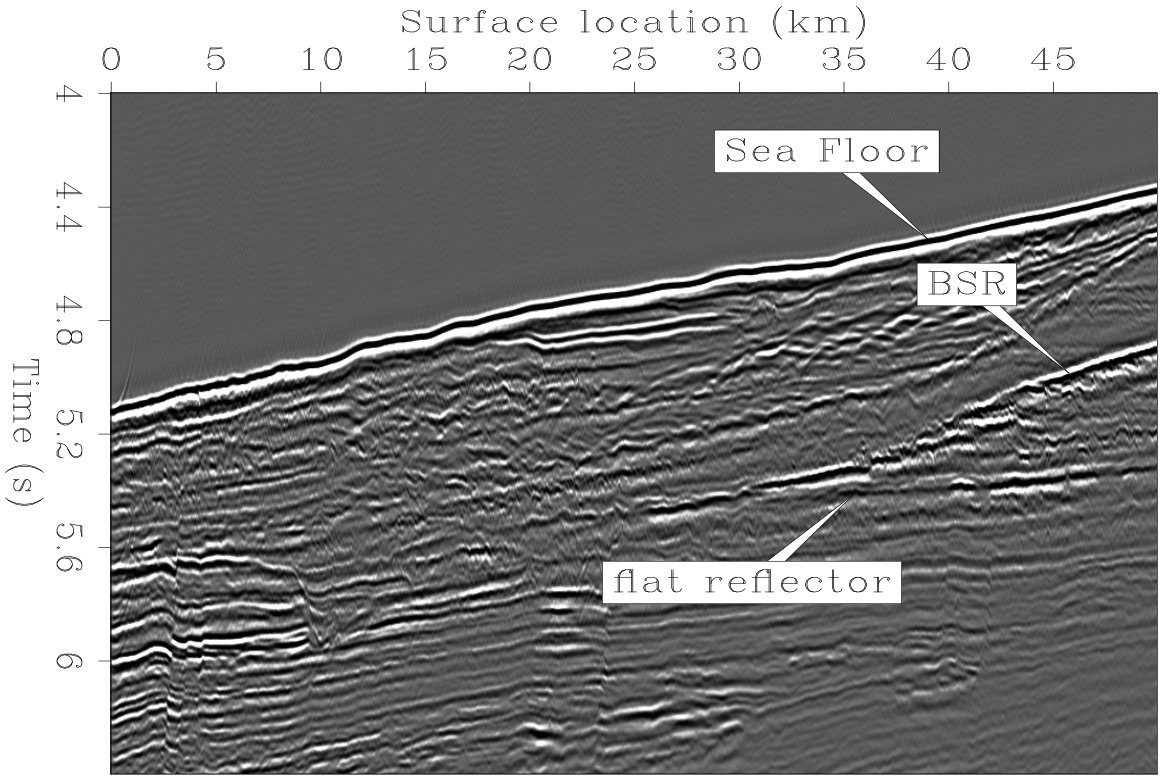

Figure 3: The stacked section after Kirchhoff migration. mamta2-Kir-hydrate-paper-ann [CR]

REFERENCES

Biondi, B., and Palacharla, G., 1995, 3-D prestack depth migration of common-azimuth data: SEP–**84**, 11–24.

Claerbout, J. F., 1984, The craft of wavefield extrapolation: SEP–**40**, 230–308.

Ecker, C., 1998, Seismic characterization of methane hydrates structures: SEP, **96**.

Lumley, D. E., 1993, Kirchhoff prestack impedance inversion: A gas reservoir pilot study: SEP–**77**, 211–230.

Prucha, M. L., Biondi, B. L., and Symes, W. W., 1999, Angle-domain common image gathers by wave-equation migration: SEP–**100**, 101–112.

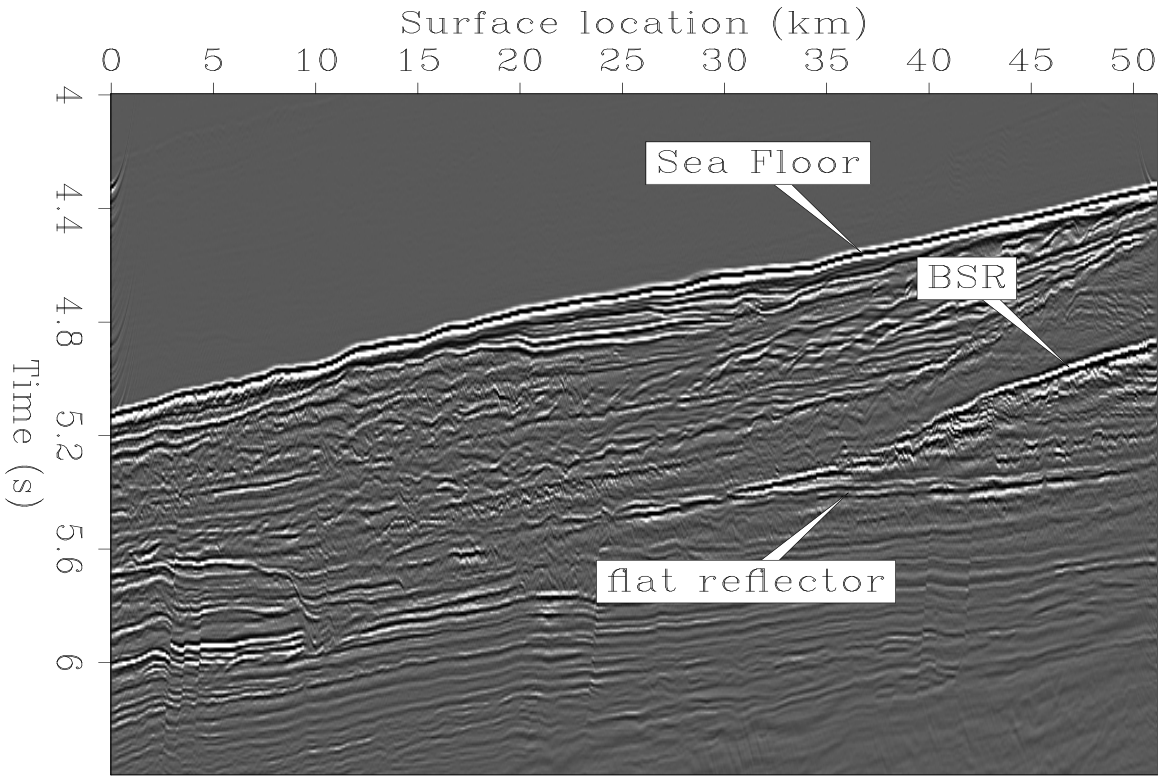

Figure 4: Wave-equation migration. mamta2-Wave-ann [CR]

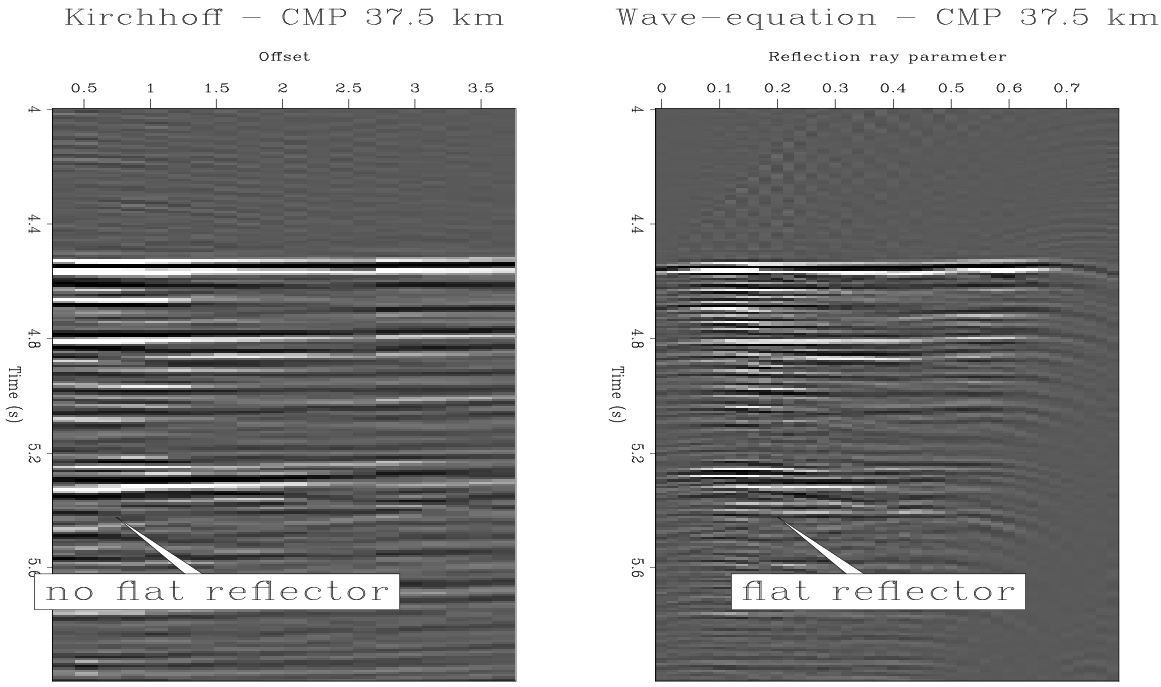

Figure 5: Common midpoint gather at 37.5 km shows the flat reflector on the right section but not on the left section. mamta2-AVO-37.5-ann [CR]

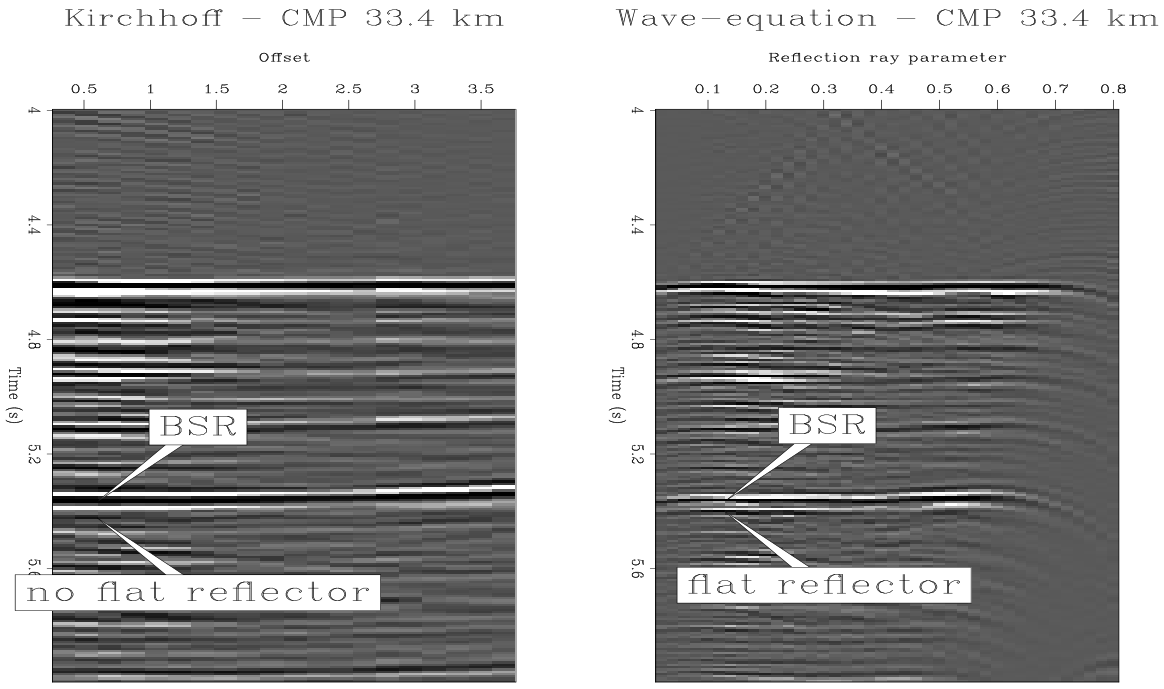

Figure 6: Common midpoint gather at 33.4 km. Right image shows resolved BSR and the flat reflector at around 5.4 sec. Not visible on the left. mamta2-AVO-33.4-ann [CR]